Absolute measurements and calculations of dielectronic recombination with metastable He-like N, F, and Si ions

L. H. Andersen, G-Y. Pan,* and H. T. Schmidt
Institute of Physics and Astronomy, Aarhus University, DK-8000 Aarhus C, Denmark

N. R. Badnell and M. S. Pindzola
Department of Physics, Auburn University, Auburn, Alabama 36849
(Received 18 November 1991)

Measurements and calculations of the rate coefficient $\langle v\sigma \rangle$ for dielectronic recombination associated with He-like ions of nitrogen, fluorine, and silicon are reported for electron energies between 0 and 27 eV. In this energy region, no resonances are associated with excitation of the $1s^2$ ground state, however, the metastable states $1s2s(^1S)$ and $1s2s(^3S)$ contribute with very large rate coefficients. The population of the $1s2s(^3S)$ metastable state was determined by an independent x-ray measurement. We performed calculations in the *LS*-coupling and intermediate-coupling approximations for dielectronic recombination from the initial ^3S and ^1S states. For the ^3S initial state, a comparison on an absolute scale between theory and experiment is presented. We find good agreement with *LS*-coupling calculations for $N^{5+}(^3S)$, one exception being a structure observed below the ^1S and ^3P threshold. For $Si^{12+}(^3S)$, the intermediate-coupling calculation reproduces the data fairly well. In the case of $F^{7+}(^3S)$, we find discrepancies with both the *LS*- and intermediate-coupling calculations at low energy and just below the ^1S and ^3P thresholds. The contribution from the initial $1s2s(^1S)$ state is important only for N^{5+}. Here, the experimental data are in excellent agreement with the theory if the ^1S metastable fraction is assumed to be about 1%.

PACS number(s): 34.80.Kw

I. INTRODUCTION

From a practical point of view, the importance of dielectronic recombination (DR) in various plasma conditions has been known for a long time. DR often results in the emission of x rays, which can be an important diagnostic tool, but it can also result in a major energy loss from hot plasmas. From a theoretical point of view, DR represents a demanding problem involving many resonance states with individual decay properties. In the particular case of metastable He-like ions, the theory has generally reached a level where it can reproduce the experimental data, except in some regions of energy where the DR cross section is sensitive to couplings between various doubly excited states. The experimental evidence for such couplings will be considered in the present paper.

It is a challenge to measure recombination between free electrons and ions at a well-defined relative energy. The cross sections connected with recombination are normally quite small, and hence signals due to electron capture from atoms or molecules present in the experimental setup may easily dominate the true recombination signal originating from the target of free electrons. If the vacuum conditions are modest, as they were in the first generation of experiments [1–3], intense sources of monoenergetic electrons are needed to obtain data with reasonable statistics. A very compressed electron beam as a target may, however, deteriorate the energy resolution. To achieve good energy resolution, the electron target has to be relatively thin, and, as a consequence, the vacuum conditions good ($\approx 10^{-11}-10^{-12}$ Torr).

With the development of electron coolers for ion-storage rings, the experimental situation has indeed improved. With these devices, electrons and ions are merged over a length of typically 1 or 2 m. They operate under ultrahigh vacuum conditions, and it is therefore possible to obtain a good energy resolution and at the same time sufficiently high electron densities to achieve a satisfying signal. DR measurement with intrashell excitations ($\Delta n = 0$) [4,5] and with $\Delta n > 0$ have been performed [6,7] by this method. DR data with highly charged ions are also being produced by the electron-beam ion-source (EBIS) and the electron-beam ion-trap (EBIT) experiments [8,9]. It is now possible to test the various theoretical approaches to a high degree. Due to a rather narrow energy resolution in the experiments, the magnitude of the cross section for individual resonances, as well as information of spectroscopic nature, are available from the experiments.

At Aarhus University, we built a device to serve as a prototype for a future electron cooler at the heavy-ion storage ring ASTRID. The cooler also serves as a target of electrons for studies of collisions between low-energy electrons and highly charged ions. In this paper, we present new DR data associated with He-like ions obtained with this electron target. We compare the experimental results with isolated-resonance distorted-wave calculations performed in the *LS*-coupling and intermediate-coupling (IC) approximations.

Dielectronic recombination is a resonant process in which an incoming electron excites an electron present on the ion. It thereby loses energy and becomes bound to the ion provided the initial kinetic energy is less than the excitation energy. In this way, doubly excited ionic states are created. If these states decay radiatively, the electron remains on the ion, and the DR process is completed. If the doubly excited states decay via autoionization, the process results in a resonance in the elastic- or interelastic-scattering cross section. The DR process can be presented by

$$X^{q+}+e^{-}\rightarrow(X^{(q-1)+})^{**}\rightarrow(X^{(q-1)+})^{*}+h\nu \ . \quad (1)$$

If the core-excitation energy is ΔE and the initial kinetic energy of the electron in the ion rest frame is E_r, then for capture to the state nl, energy conservation yields

$$E_r+E_{nl}=\Delta E \ , \quad (2)$$

where E_{nl} is the binding energy of the state designated nl. In principle, an infinite but convergent series of resonances is then found at energies E_r satisfying Eq. (2). In practice, external analyzing fields will limit the number of contributing Rydberg levels and make the number of contributing resonances finite.

DR with ground-state He-like ions may occur due to excitation of one of the two 1s electrons. Measurements on DR, or the equivalent process in ion-atom collisions called resonant transfer and excitation (RTE) for ground-state He-like systems, have been reported by several groups [8–10]. In general, the experimental data covering ions with charge states up to 90 are in good agreement with the existing theory.

When the ions are in the metastable $1s2s(^{1,3}S)$ states, not only may the 1s electron become excited, but the much more loosely bound 2s electron may be excited to the 2p state. In three previous papers [4,5,11] we have reported on dielectronic recombination associated with the $2s\rightarrow2p$ excitation from metastable He-like $C^{4+}[1s2s(^{1,3}S)]$ and $O^{6+}[1s2s(^{1,3}S)]$. It was found that the DR cross sections for the metastable ions may be extremely large, in the order of 10^{-15} cm^2, for some of the individual resonances [11,12]. The fast radiative core transition of the $1s2p(^1P)nl$ state to the $1s^2(^1S)nl$ state is largely responsible for this.

Although most of the resonances were well represented as isolated resonances, of special interest was the discovery that some measured resonances for O^{6+} were not well predicted by the theory [11,12]. This was interpreted [11,13] as being due to the presence of low-lying $1s2s(^1P)nl$ ($n=7$, 8, 9, or 10) resonances which coupled to high-lying $1s2s(^1S)n'l'$ and $1s2p(^3P)n''l''$ ($n',n''>20$) resonances. This allowed the ^1S and ^3P cores to radiatively stabilize and thus increase the DR cross section. The precise coupling mechanism was not clear, although bound-bound electrostatic configuration interaction was ruled out [11]. However, in the case of C^{4+}, theory and experiment were found to be in good agreement. In order to study the appearance of the large resonance structures more systematically, we performed a new series of measurements with He-like N, F, and Si ions. This allowed us to study the transition from low-Z ions, where the LS-coupling approximation is valid, to ions with larger Z where the spin-orbit interaction becomes more important.

The rate coefficients quoted in the experimental papers [4,5] were not on an absolute scale due to the lack of precise knowledge about the initial-state population of the ion beam. This, in turn, limited the comparison between theory and experiment to a relative level (a very fruitful comparison could still be made, however). It is well established that when an ion penetrates a thin foil, the foil K x-ray yield is strongly dependent on the number of K holes in the ion beam [14,15]. This allowed us to determine the fraction of 1s2s metastable states in the ion beam so that we can present a comparison between the DR data and the theory on an absolute scale.

II. EXPERIMENT

A. Recombination measurements

The dielectronic-recombination results, which are reported here, were obtained at the EN-Tandem accelerator at the Institute of Physics and Astronomy, Aarhus University. 1.25 MeV/amu ions were passed through a thin-C foil (5 μg/cm^2). The He-like ions exiting the foil were then magnetically selected and merged with an almost monoenergetic beam of electrons with essentially the same speed as the ion beam. Different relative energies were obtained by varying the electron-beam energy which was around 800 eV. The electron beam had an almost constant current density over a diameter of 1 cm and was guided by a magnetic field of about 150 G, which was applied to compensate for the space-charge field due to the charged electrons. Both the ion and electron beam could be modulated at a frequency of 2 MHz so that electrostatic pickup plates could monitor the position of the two beams in the interaction region. Thereby the two beams were brought into full overlap. Figure 1 shows the experiment schematically. Details for the experimental apparatus may be found in previous publications [4,5].

The recombination process was identified by counting ions that had collected one electron after their passage through the interaction region. The background contribution in the DR measurements due to capture in the rest gas was found via a smooth fit to the yield of ions (of charge state $q-1$) at energies outside the resonances. The electron beam used by this method was run in the dc mode. Alternatively, for radiative recombination measurements mainly, the electron beam was turned on and off (ac mode) by changing the anode voltage between 0 and -2 kV at a frequency between 100 and 500 Hz. At the anode voltage of -2 kV, the electron beam was stopped, and the background yield was measured.

Since very small relative energies were considered, the energy spread in the electron beam could not be neglected. Instead of the cross section, we determined the rate coefficient which was defined as

$$\langle v\sigma\rangle=\frac{N^{(q-1)+}-N_0^{(q-1)+}}{N^{q+}}\frac{v_i}{L\rho\epsilon} \ , \quad (3)$$

where q is the total charge of the incoming ion, L is the length of the merged section, ϵ is the ion-detection efficiency, v_i is the ion velocity, and ρ is the electron den-

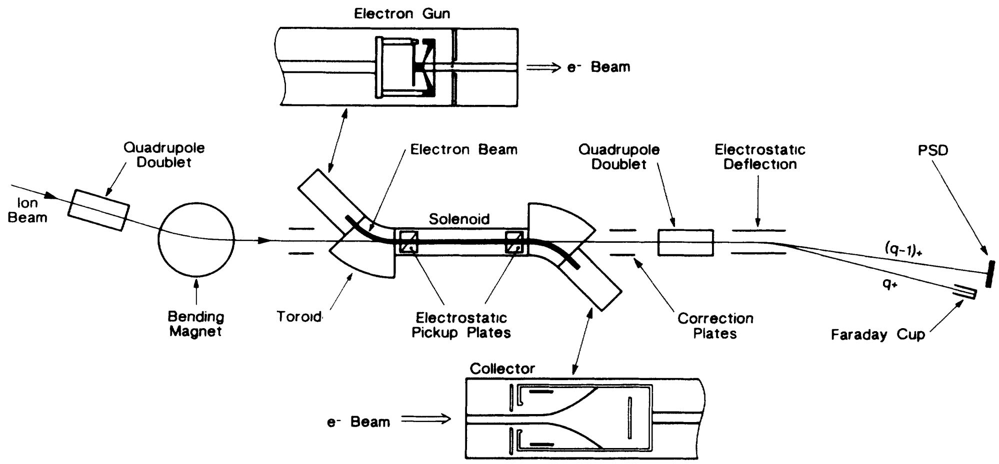

FIG. 1. The experimental setup. PSD denotes a position-sensitive detector.

sity which typically was $5\times10^7/\text{cm}^3$. In Eq. (3), N^{q+} is the number of incoming ions in *any* state. In our first report on DR with He-like ions [4,5], the metastable fractions were unknown, and only relative values for the singlet and triplet initial states were obtained. We have now measured the ^3S population by an independent technique.

B. Metastable fraction determination

The $1s2s$ metastable fraction in the ion beam was determined using a thin, evaporated Al layer on a carbon foil. We used Al thicknesses between 10 and 50 Å. The emitted Al K x rays were detected by a Si(Li) x-ray detector mounted at 90° with respect to the beam direction. The method utilizes the fact that the yield of emitted target K x rays reflects the number of K holes in the ion beam. That is, a constant yield is obtained for ions with no K holes (see Fig. 2). For ions with one K hole (H-like), a significant increase is observed due to K-to-K electron transfer. It is assumed that the $1s^2(^1S)$ component of the He-like beam results in the same Al K x-ray yield as do

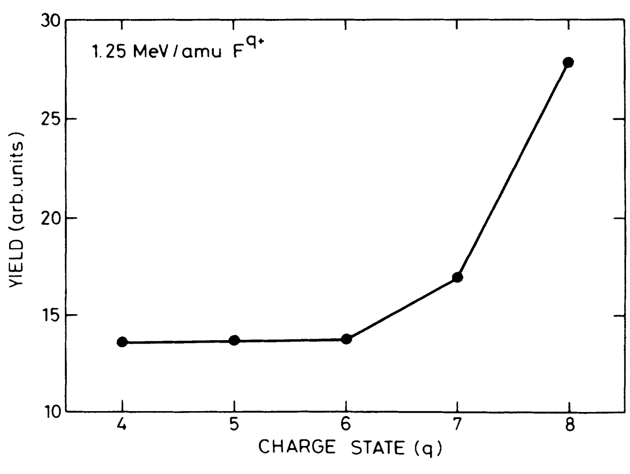

FIG. 2. The yield of Al K x rays as a function of the charge state of the incoming fluorine ion. The ion energy is 23.75 MeV corresponding to 1.25 MeV/amu.

the Li-, Be-, and B-like ions. Further, it is assumed that ions in the metastable $1s2s(^1S)$ and $1s2s(^3S)$ states produce the same yield as do ions in the H-like $1s$ state. The metastable fraction *at the Al-foil target* is then simply given by

$$f(s\,1s2s)=\frac{Y_{(\text{He-like})}-Y_0}{Y_{(\text{H-like})}-Y_0}\ , \tag{4}$$

where Y_0 is the constant yield obtained with beams without holes in the K shell.

For normalization, the ion beam was passed through a 200-Å gold foil and collected in a Faraday cup. The current from the Faraday cup as well as backscattered ions from the foil were used for the normalization. The two methods were in agreement to within a few percent.

In Fig. 2, we show the K x-ray yield obtained with five different fluorine ions. Evidently, the yield for ions with no K holes is nearly constant. The increase due to the presence of K holes is seen for the H-like ions ($q=8$) and the metastable He-like ions ($q=7$).

For the ion beams used in this work, the lifetimes of the ^3S state [16] were much longer than the ion-flight time from the place of production to the foil target. The lifetimes of the ^1S states [17] are significantly shorter than that of the ^3S states, and a reduction due to the exponential decay was taken into account. In the case of N^{5+}, the $1s2s(^1S)$ population was reduced by a factor of 0.58 due to the finite lifetime (1.06 μsec) and the travel time of 0.57 μsec. To obtain the ^3S population, we assumed the ^1S initial population at the poststripper foil to be one-third of the ^3S population (i.e., statistical population). Thus, $f(^3S)=f(1s2s)/(1+0.58/3)=0.84f(1s2s)$ for N^{5+}. For F^{7+} and Si^{12+}, we used $f(^3S)=f(1s2s)$ due to the short lifetimes of the ^1S states for these beams. Taking into account the ion-flight time (0.73 μsec) to the electron target, we obtained the metastable fractions listed in Table I. For the sake of completeness, we also list the values for C^{4+} and O^{6+}, the DR data of which have been published before [4,5,11]. For O^{6+}, these values are in good agreement with the values that resulted from a comparison with the DR calculation [11]. The previous C^{4+}

TABLE I. Fractions of metastable states (in %) in the ion beams at the electron target. The ^1S-state population was estimated to one-third of the ^3S population at the place of production.

State	C^{4+}	N^{5+}	O^{6+}	F^{7+}	Si^{12+}
$1s2s(^1S)$	3	2	1	0.2	0.004
$1s2s(^3S)$	16	15	20	23	12

data were obtained by stripping the ion beam in the terminal stripper gas at the tandem accelerator. This gave a considerably smaller metastable fraction than that shown in Table I (about 5–7 % for the ^3S state). This, together with a factor-of-ten error in preliminary data communicated privately, resulted in some confusion in the first analysis of the He-like DR measurements [11]. In fact, there is very good agreement between theory and experiment for the obtained metastable fractions of C^{4+}.

III. THEORY

We consider the following DR reactions for the initial metastable $1s2s(^1S)$ and $1s2s(^3S)$ states

$$\left.\begin{array}{l} 1s2s(^1S)+e^- \rightarrow 1s2p(^1P)nl \\ 1s2s(^3S)+e^- \rightarrow 1s2s(^1S)nl \\ 1s2s(^3S)+e^- \rightarrow 1s2p(^3P)nl \\ 1s2s(^3S)+e^- \rightarrow 1s2p(^1P)nl \end{array}\right\} \rightarrow 1s^2(^1S)n'l'+h\nu \ . \tag{5}$$

The energy-averaged dielectronic-recombination cross section for a given initial state i through an intermediate state j is given by

$$\sigma_{\varepsilon_0,\Delta\varepsilon}=\frac{(2\pi a_0 I)^2}{\varepsilon_0\Delta\varepsilon}\frac{\omega(j)}{2\omega(i)} \times \frac{\tau_0\sum_k A_r(j\rightarrow k)\sum_l A_a(j\rightarrow i,\varepsilon_0 l)}{\sum_h A_r(j\rightarrow h)+\sum_{m,l} A_a(j\rightarrow m,\varepsilon_0 l)} , \tag{6}$$

where ε_0 is the energy of the continuum electron, $\Delta\varepsilon$ is the energy-bin width (here typically 0.03 eV), and I is the ionization potential of hydrogen. Here, $\omega(i)$ is the statistical weight of the initial state of the N-electron ion, $\omega(j)$ is the statistical width of the doubly excited resonance state of the $(N+1)$ electron ion, and a_0 and τ_0 are the atomic units for length and time, respectively. In the denominator, which is the total decay rate of the intermediate resonance state j, the sums of the radiative rates (A_r) and the Auger rates (A_a), are over all accessible states. In the numerator, the sum over k is over all states that are stable against autoionization. The various rates entering Eq. (6) were calculated in the isolated-resonance and independent-process approximations by the use of a computer code called AUTOSTRUCTURE [18,19]. In particular, both LS- and intermediate-coupling schemes were used. The Breit-Pauli Hamiltonian used in the IC calculations included both one-body and two-body fine-structure interactions, the effective one-body spin-orbit one being dominant. Fine-structure interactions mix the $^3P_{J=1}$ and the $^1P_{J=1}$ core levels, allowing the $1s2s(^3P)nl$ resonance states to stabilize radiatively to the $1s^2(^1S)nl$-core ground level. Note that this is independent of any $^1P_{J=1}n'l'$ resonances, so the IC enhancement over the LS coupling should exist (given a high enough charge state) irrespective of the position of any low-lying $^1P_{J=1}n'l'$ resonances.

In order to compare the theory with the experimental data, we calculated

$$\langle v\sigma\rangle=\int_0^\infty \sigma(E)\left[2\frac{E}{m}\right]^{1/2}\frac{dN}{dE}(E)dE = \sum_i \sigma_{\varepsilon_0,\Delta\varepsilon^i}\int_{(i-1)\Delta\varepsilon}^{i\Delta\varepsilon}\left[2\frac{E}{m}\right]^{1/2}\frac{dN}{dE}(E)dE , \tag{7}$$

where dN/dE is the electron density that is given in terms of the relative velocity distribution $f(\mathbf{v})$:

$$\frac{dN}{dE}=\frac{v}{m}\int_\Omega f(v)d\Omega . \tag{8}$$

Due to the longitudinal acceleration of the electron beam, the relative velocity spread in the experiment cannot be characterized by a single temperature. The velocity distribution was characterized by a product of two Maxwell distributions, one accounting for the transverse electron motion and one for the longitudinal motion. The velocity distribution then becomes

$$f(v)=\frac{m}{2\pi kT_\perp}e^{-mv_\perp^2/2kT_\perp}\left[\frac{m}{2\pi kT_\parallel}\right]^{1/2}e^{-m(v_\parallel-\Delta)^2/2kT_\parallel} , \tag{9}$$

where $v_\perp$ and $v_\parallel$ are the electron-velocity components perpendicular and parallel to the ion-beam direction, respectively, and Δ is the detuning velocity that defines the relative energy $(\frac{1}{2}m\Delta^2)$. It was found that the measured shape of individual DR resonances contains information that could easily yield the transverse energy spread $kT_\perp$ as well as the longitudinal energy spread $kT_\parallel$. The two temperatures were $kT_\perp=0.15$ eV and $kT_\parallel=0.001$ eV in the dc mode and $kT_\parallel=0.002$–0.003 eV in the ac mode.

IV. RESULTS

In the present study, we continued our investigation of DR with metastable He-like ions. Theoretical [11] as well as experimental [4,5] results for C^{4+} and O^{6+} have been presented before. Two problems remained after the first measurements. One was the problem of unknown metastable fractions in the ion beam. Another was the unexpected large resonances near the $1s2s(^1S)$ and $1s2p(^3P)$ limits for O^{6+}. To elucidate these questions, we report here on DR with metastable He-like ions of N, F, and Si with known fractions of the metastable ^3S state.

In Fig. 3 is shown the rate coefficient $\langle v\sigma\rangle$ [see Eq. (3)] for 1.25 MeV/amu N^{5+}. The energy region is from 0

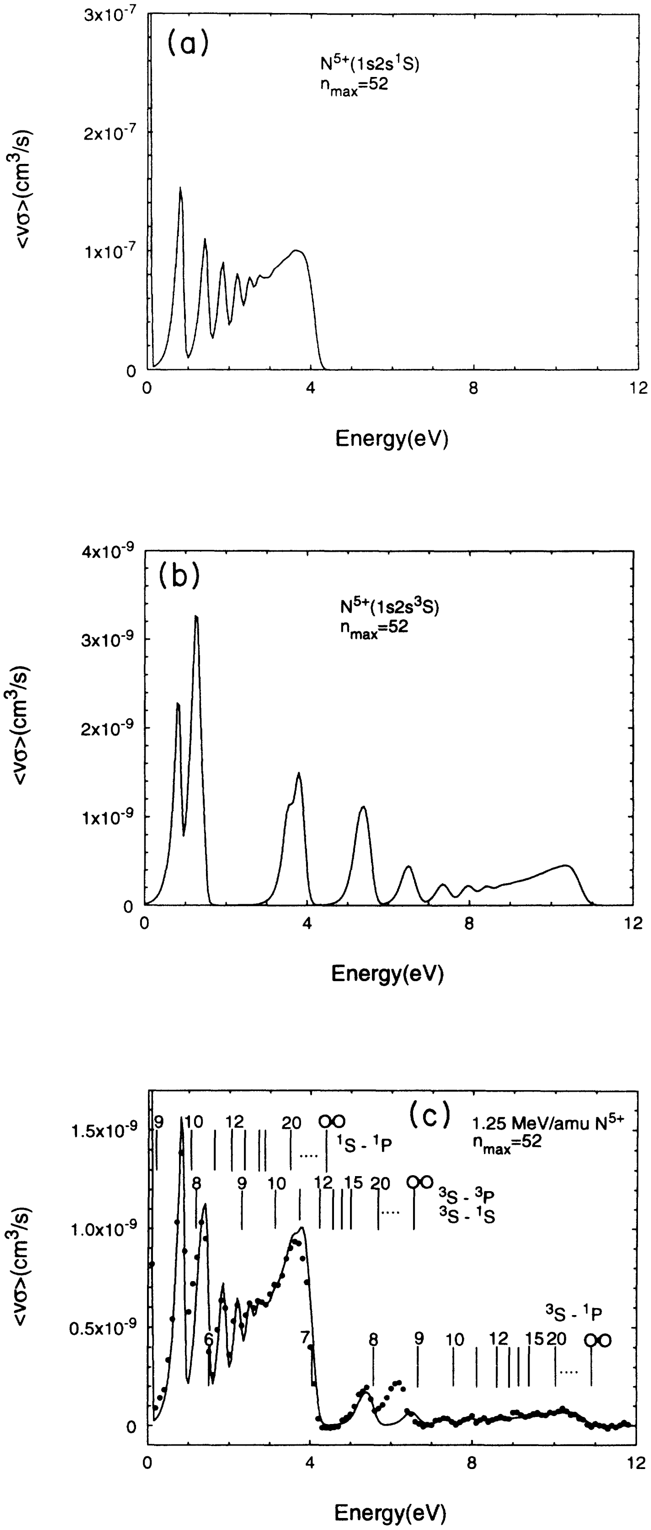

FIG. 3. The rate coefficient $\langle v\sigma \rangle$ as a function of electron energy for 1.25 MeV/amu N^{5+}. (a) *LS*-coupling calculation for the ^1S initial state. (b) *LS*-coupling calculation for the ^3S initial state. (c) The experimental data together with the *LS*-coupling calculations. The ^1S population was assumed to be 0.8% and the ^3S population 15%. The temperatures $kT_\perp = 0.15$ eV and $kT_\parallel = 0.001$ eV were used in the calculation of $\langle v\sigma \rangle$.

to 12 eV where all DR resonances associated with the $2s \rightarrow 2p$ excitation are found. The position of the individual resonances (E_n) was calculated according to Eq. (2)

$$E_n = \Delta E - \frac{q^2 13.6 \text{ eV}}{n^2} , \tag{10}$$

where ΔE was obtained from the calculation of Drake [20]. In principle, one should observe an infinite series of resonances associated with each individual core excitation; however, the presence of strong analyzing fields acting on the ions outside the interaction region in the experiment reduces the maximum number of Rydberg states to a finite value n_{max}. For N^{5+}, F^{7+}, and Si^{12+}, n_{max} was equal to 52, 68, and 97, respectively.

Since N^{5+} is the only ion considered here that contains a significant population in the initial $1s2s(^1S)$ state, we show in Fig. 3(a) the *LS*-coupling calculation for DR from the initial ^1S state. The $2s(^1S)$-to-$2p(^1P)$ excitation energy is 4.28 eV. Individual resonances, with a series limit at this energy, are recognized. Figure 3(b) shows the result of the *LS*-coupling calculation for the initial ^3s state. Here, the series limit for the ^3S-to-^1P excitation is at 10.91 eV. The corresponding resonances are clearly seen. Resonances associated with the ^3S-to-^1S (6.63 eV) and ^3S-to-^3P (6.52 eV) excitations are much weaker. By comparing Figs. 3(a) and 3(b), we see that the DR cross sections associated with the $1s2s(^1S)$ initial state are about two orders of magnitude larger than that associated with the $1s2s(^3S)$ state. The DR calculations were folded with the velocity distribution $f(\mathbf{v})$ with the temperatures $kT_\perp = 0.15$ eV and $kT_\parallel = 0.001$ eV. In Fig. 3(c) we show the experimental data together with the result of the calculation based on 0.8%-^1S and 15%-^3S initial populations. The ^3S population was that found from the x-ray measurement, and the ^1S initial population was fitted to the experimental data. The obtained ^1S population is somewhat less than the statistical prediction of 2%.

The merged-beams method used in the present work offers a very good energy resolution at low relative energies. In Fig. 4 we show the results for N^{5+} at relative energies around 0 eV. Negative energies correspond here to the situation where the electrons are slower than the ions, while positive energies correspond to the case where the electrons are faster than the ions. As expected, we see a symmetric rate coefficient with respect to $E_r = 0$. Note the asymmetric shape of the DR resonances which results from the unique velocity distribution [Eq. (9)] with very different parallel and perpendicular temperatures. In the figure we show the partial contributions from the initial ^1S and ^3S states. The sum curve (theory) reproduces the experiment very well. In the calculation, we did not include radiative recombination which mainly contributes at low energy. The radiative-recombination rate coefficient at $E_r = 0$ is estimated to contribute by less than 2% at $E_r = 0$. A rate coefficient of about 7×10^{-11} cm^3/s was obtained experimentally with C^{5+} [21].

The overall agreement between experiment and the isolated resonance theory is very good except for one region at around 6 eV which is just below the ^3P and ^1S series limits [see Fig. 3(c)]. Here the data exhibit a clear peak

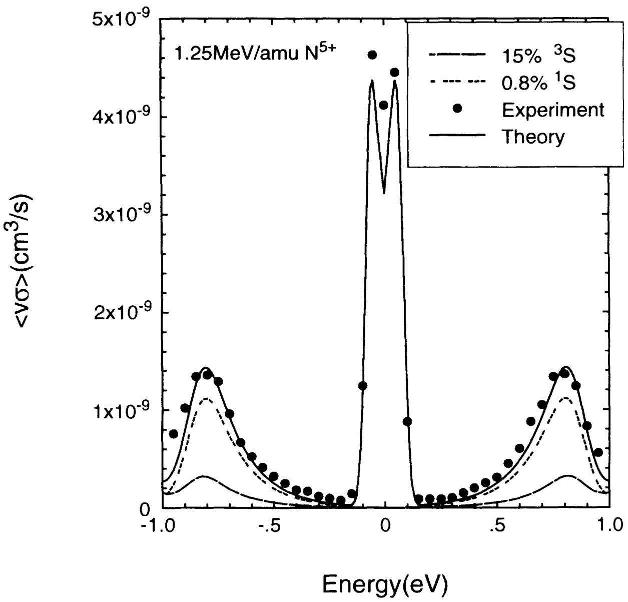

FIG. 4. The rate coefficient for N^{5+}. The dotted curve is the theoretical contribution for 0.8% initial ^1S, the dashed curve is the theoretical contribution for 15% initial ^3S. The solid curve is the sum of the two contributions. The temperatures $kT_\perp = 0.15$ eV and $kT_\parallel = 0.002$ eV were used in the calculation of $\langle v\sigma \rangle$.

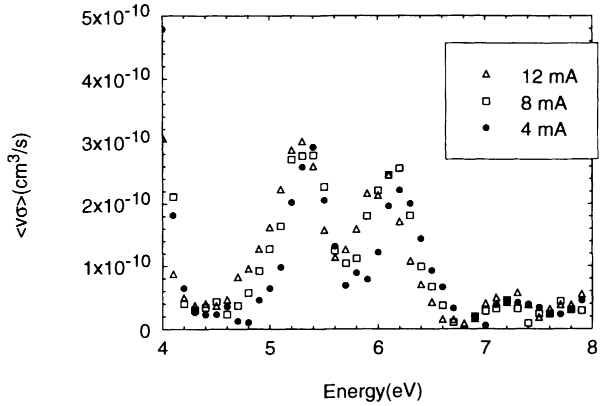

FIG. 5. The rate coefficient as a function of energy for 1.7 MeV/amu N^{5+}. Data are shown for three different electron currents 4, 8, and 12 mA.

that is not predicted by the *LS*-coupling calculation. The result of the IC calculation does not differ from that of the *LS*-coupling calculation. At this point, we note that any mixing between the high Rydberg members of the ^3Pnl and ^1Snl series with the ^1P $(n=9)$ level may cause an enhancement in this energy region due the strong $1s2p(^1P) \rightarrow 1s^2(^1S)$ radiative transition. The same observation was made for O^{6+} [11]. In addition to the unpredicted structure below the ^3P and ^1S series limits, the experimental data for O^{6+} exhibited an enhancement over the theory also at the $^3S \rightarrow {}^1P$ $(n=7)$ resonance. In the case of O^{6+}, the IC-approximation calculation made a very small improvement over the *LS*-approximation calculation just below the ^3P and ^1S series limits.

The calculations do not take into account any effects of perturbing external electric fields which may be present in the interaction region in the order of a few V/cm. The enhanced peaks could therefore in principle be due to field-induced stabilization of the $1s2p(^3P)nl$ and $1s2s(^1S)nl$ Rydberg states. To examine this, we measured $\langle v\sigma \rangle$ in the energy region from 4 to 8 eV where the extra resonance structure was observed for N^{5+}. We performed the measurement with three different electron densities corresponding to an electron beam of 4, 8, and 12 mA. As seen from Fig. 5, there appears to be little difference between the spectra obtained with the different electron densities and thereby different electric fields produced by the space charge. There may be small shifts in the apparent position of the resonances due to the change in the space-charge potential. Further, the widths of the peaks may change slightly due to changes in the electron temperatures with changing electron density.

When comparing the data from Fig. 5 with those of Fig. 3(c), it is evident that the relative height of the two peaks has changed. The data of Fig. 5 were taken at 1.7 MeV/amu, and the data of Fig. 3(c) were taken at 1.25 MeV/amu. Different strength of the strong charge-state analyzing field after the interaction region was used with correspondingly different values of n_{max} (49 and 52). The change due to stripping of Rydberg states in the analyzer field was calculated to be about 2–3 %. The metastable fractions may have changed when going from 1.25 MeV/amu to 1.7 MeV/amu. However, the structure, displayed in Fig. 5, is *above* the $^1S \rightarrow {}^1P$ series limit and should not alter the relative height of the two peaks since they presumably both result from the initial ^3S state. The relative reduction around $E_r = 6.2$ eV of about 20% is at this moment not understood.

In Fig. 6 we show the results for F^{7+}. The experimental data are compared with both the *LS*- and IC-approximation calculations. It is assumed that there is a small fraction of 0.04% ^1S metastable states in the beam. As in the case of N^{5+}, we find that the ^1S population in the ion beam is less than statistically populated. The fraction of triplet states was set equal to 23%, as measured by the independent x-ray measurement.

For F^{7+}, the IC-approximation calculation reproduces the data somewhat better than the *LS*-coupling calculation does. The large peak below the ^3P and ^1S series limits, however, is still not fully accounted for. Note also that the peak at 4 eV and that at about 6.5 eV in the experimental data have about the same magnitude. If they were members of the same series ($n=8$ and 9 of the ^3S-to-^1P transition), they should decrease with increasing energy roughly as $1/E$ [see Eq. (6), and also the calculated rate coefficient in Fig. 6]. We interpret this as sign of an enhancement of the DR signal around $n=9$. An even larger enhancement is observed at $n=10$.

In Fig. 7 we show the F^{7+} data together with the LS-coupling calculations in the energy range from 0 to 1.5 eV. The solid curve is the calculation of the ^3S metasta-

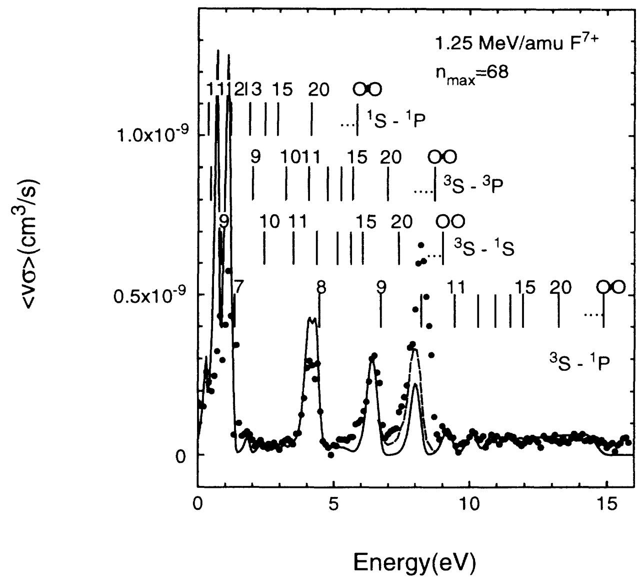

FIG. 6. The rate coefficient $\langle v\sigma \rangle$ as a function of electron energy for 1.25 MeV/amu F^{7+}. Shown are the experimental data together with the *LS*- (full curve) and intermediate-coupling (dashed curve) calculation. The temperatures $kT_{\perp}=0.15$ eV and $kT_{\parallel}=0.001$ eV were used in the calculation of $\langle v\sigma \rangle$. The ^1S population was assumed to be 0.04% and the ^3S population 23%.

ble contribution (23%), and the dashed curve results from 0.04% ^1S initial metastable states. In the figure we indicate by bars the resonance positions as obtained from Eq. (10) for the initial ^1S and ^3S states. We can identify the various resonances from their positions. (Bear in mind that the resonance position for the data obtained by the applied experimental technique is midway down on the high-energy side of the observed resonances [5].) Further, it must be born in mind that the resonances indicated by bars are calculated from the Rydberg formula without quantum defects. The $1s2s(^3S)\rightarrow 1s2p(^1P)$ $(n=7)$ resonance is calculated to be at 1.29 eV from the Rydberg formula. A quantum defect of 0.0375 is required to bring it in agreement with the resonance observed at 1.15 ± 0.01 eV. As seen from the figure, the agreement between theory and experiment is within a factor of 2 to 3 for the ^3S initial state. For the ^1S initial state, we did not know the exact metastable fraction, and a value of 0.04% was estimated from the comparison between the experimental and the calculated rate coefficients.

Using the measured metastable fraction of the ^3S state and the fitted ^1S metastable fractions, we find good agreement between theory and experiment in the case of N^{5+} at low energy. Similar agreement is found for C^{4+} and O^{6+}. Theoretically, we would expect the agreement between theory and experiment to improve with increasing charge. But for F^{7+}, the theoretical results are a factor of 2 or 3 greater than the experimental cross sections if we use the measured ^3S metastable fraction of 23%. Indeed, taking into account the enhancement of the DR cross section near $n=9$ and $n=10$ not described by theory (see Fig. 6), then the theoretical results are arguably too large over the entire spectrum, in stark contrast with the case of N^{5+} (see Fig. 3). If we were to normalize theory to experiment around the $n=7$ cross section, based on the agreement for lower charge ions, this would correspond to a ^3S fraction of about 10%. This would leave room for a small enhancement of the DR cross section around $n=8$ and for the argued enhancement around $n=9$ and 10.

For N^{5+} and F^{7+} (as well as for C^{4+} and O^{6+}), we see that the DR rate coefficient *above* the $1s2s(^1S)$ and $1s2p(^3P)$ series limits is very small. This is due to a strong coupling between the ^3P and ^1S continua and the $1s2p(^1P)nl$ resonances, which causes the resonances to autoionize rather than stabilize by radiation.

As our last example of DR with metastable He-like ions, we considered Si^{12+}. In Fig. 8 are shown the experimental data together with both the *LS*- and IC-approximation calculation. In the calculations, we used 12% for the ^3S initial state as obtained from the x-ray measurement (0% for ^1S). For Si^{12+} there is a large difference between the results of the two coupling schemes. The rapid change in the DR spectrum observed when going from F^{7+} to Si^{12+} originates from the Z^9 dependence of the $1s2p(^3P)\rightarrow 1s^2(^1S)$ radiative rate due to spin-orbit mixing. Due to the low ion current obtained with Si^{12+} and the frequent change in poststripper foils, some scatter appears in the experimental data. Within the rather large (mainly statistical) uncertainty of the experimental data, the IC calculation reproduces the data. We see a new Rydberg series associated with the $^3S_0\rightarrow {}^3P_1$ excitation. The $^3P_{J=1}$ core is now able to radiate to the $1s^2(^1S_{J=0})$ ground state due to the spin-orbit

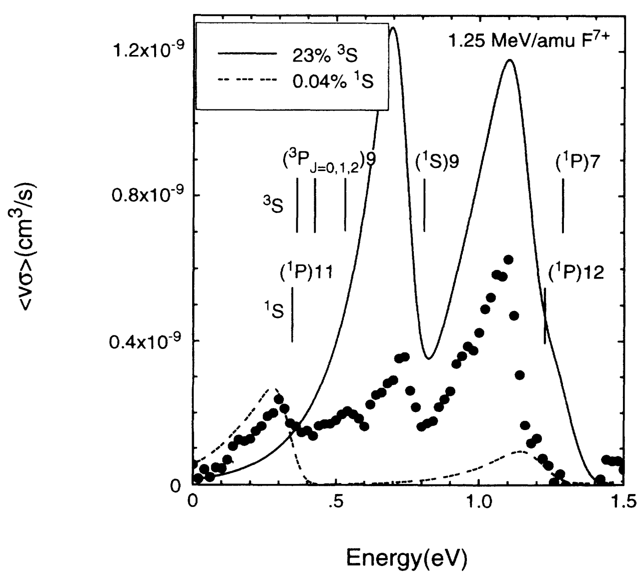

FIG. 7. The rate coefficient $\langle v\sigma \rangle$ as a function of electron energy for 1.25 MeV/amu F^{7+}. The full curve is the *LS*-coupling-calculation result, assuming 23% metastable ^3S states in the beam. The dotted curve is the same calculation for 0.04% metastable ^1S states in the beam.

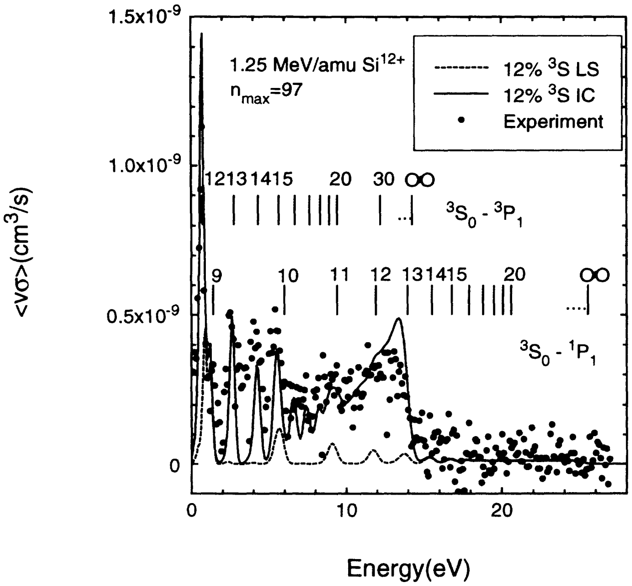

FIG. 8. The rate coefficient $\langle v\sigma \rangle$ as a function of electron energy for 1.25 MeV/amu Si^{12+}. Shown are the experimental data together with the *LS*-coupling calculation (dashed curve) and the IC calculation (full curve). The temperatures $kT_\perp = 0.15$ eV and $kT_\parallel = 0.003$ eV were used in the calculation of $\langle v\sigma \rangle$. In the calculations, the ^1S population was assumed to be 0% and the ^3S population 12%.

interaction. This is not the case for the $J=0$ and 2 fine-structure levels. The differences between experiment and theory observed for the other He-like ions below the $1s2s(^1S)$ and $1s2p(^3P)$ series limits are not seen for Si^{12+}, presumably because of the strength of the spin-orbit interaction.

V. CONCLUSION

We find that dielectronic recombination associated with the metastable $1s2s(^3S)$ state of low-*Z* ions (C^{4+}) can be calculated with high accuracy in the *LS*-coupling approximation. For high-*Z* ions (Si^{12+}), the IC calculation reproduces the experimental data. For ions with medium-high *Z*, such as N^{5+} and O^{6+}, we find the overall agreement between *LS*-coupling theory and experiment to be good. However, we find structures, mainly below the ^3P and ^1S series limits, which are not accounted for theoretically, in the isolated resonance approximation. It was verified that the structures do not result from the external electric field produced by the space charge. For F^{7+}, there is good agreement between theory and experiment above the ^3P and ^1S thresholds. Below these thresholds we find significant deviations between theory and experiment. The differences are believed to be due to couplings between the $1s2p(^1P)nl$, $1s2s(^1S)n'l'$, $1s2p(^3P)n''l''$, and $1s2s(^3S)\epsilon l'''$ configurations. But, the precise details remain unexplained.

All the observed DR resonances associated with the ^1S initial state were well accounted for theoretically. By comparing theory and experiment we extracted the ^1S metastable fraction. The obtained metastable fractions were within expectations.

ACKNOWLEDGMENTS

We would like to thank Niels Rud and Søren B. Hansen for their kind assistance during the x-ray measurements. The experimental work was supported by the Danish National Council of Science, the Carlsberg Foundation and Ib Henriksen's Foundation and the theoretical work by the Office of Fusion Energy, U.S. Department of Energy under Contract No. DE-FG05-86ER53217 with Auburn University.

*Permanent address: Institute of Physics, Chinese Academy of Science, Beijing, People's Republic of China.

[1] P. F. Dittner, S. Datz, P. D. Miller, C. D. Moak, P. H. Stelson, C. Bottcher, W. B. Dress, G. D. Alton, N. Neskovic, and C. M. Fou, Phys. Rev. Lett. **51**, 312 (1983).

[2] D. S. Belic, G. H. Dunn, T. J. Morgan, D. W. Mueller, and C. Timmer, Phys. Rev. Lett. **50**, 399 (1983).

[3] J. B. A. Mitchell, C. T. Ng, J. L. Forand, D. P. Levac, R. E. Mitchell, A. Sen, D. B. Miko, and J. W. McGowan, Phys. Rev. Lett. **50**, 335 (1983).

[4] L. H. Andersen, P. Hvelplund, H. Knudsen, and P. Kvistgaard, Phys. Rev. Lett. **23**, 2656 (1989).

[5] L. H. Andersen, J. Bolko, and P. Kvistgaard, Phys. Rev. A **41**, 1293 (1990).

[6] G. Kilgus *et al.*, Phys. Rev. Lett. **64**, 737 (1990).

[7] J. A. Tanis *et al.*, Nucl. Instrum. Methods B **56/57**, 337 (1991).

[8] R. Ali, C. P. Bhalla, C. L. Cocke, and M. Stockli, Phys. Rev. Lett. **64**, 633 (1990).

[9] D. A. Knapp *et al.*, Phys. Rev. Lett. **62**, 2104 (1989).

[10] W. G. Graham *et al.*, Phys. Rev. Lett. **65**, 2773 (1990).

[11] N. R. Badnell, M. S. Pindzola, and D. C. Griffin, Phys. Rev. A **41**, 2422 (1990).

[12] R. Bellantone and Y. Hahn, Phys. Scr. **42**, 650 (1990).

[13] K. Taulbjerg and J. Macek, Phys. Rev. Lett. **62**, 2766 (1989).

[14] M. Terasawa *et al.*, Phys. Rev. A **27**, 2868 (1983).

[15] K. Dybdal and N. Rud, Phys. Scr. **35**, 441 (1987).

[16] G. W. Drake, Phys. Rev. A **3**, 908 (1971).

[17] G. W. F. Drake, G. A. Victor, and A. Dalgarno, Phys. Rev. **180**, 25 (1969).

[18] N. R. Badnell, J. Phys. B **19**, 3827 (1986).

[19] N. R. Badnell and M. S. Pindzola, Phys. Rev. A **39**, 1685 (1989).

[20] G. W. Drake, Can. J. Phys. **66**, 586 (1988).

[21] L. H. Andersen and J. Bolko, J. Phys. B **23**, 3167 (1990).